

Article

Infrared Absorption Spectra, Radiative Efficiencies, and Global Warming Potentials of Newly-Detected Halogenated Compounds: CFC-113a, CFC-112 and HCFC-133a

Maryam Etminan ¹, Eleanor J. Highwood ¹, Johannes C. Laube ², Robert McPheat ³, George Marston ⁴, Keith P. Shine ^{1,*} and Kevin M. Smith ³

¹ Department of Meteorology, University of Reading, Reading RG6 6BB, UK;

E-Mails: m.etminan@pgr.reading.ac.uk (M.E.); e.j.highwood@reading.ac.uk (E.J.H.)

² School of Environmental Sciences, University of East Anglia, Norwich NR4 7TJ, UK;

E-Mail: j.laube@uea.ac.uk

³ RAL Space Department, Rutherford Appleton Laboratory, Didcot OX11 0QX, UK;

E-Mails: robert.mcpheat@stfc.ac.uk (R.M.); kevin.smith@stfc.ac.uk (K.M.S.)

⁴ Department of Chemistry, University of Reading, Reading RG6 6AD, UK;

E-Mail: g.marston@reading.ac.uk

* Author to whom correspondence should be addressed; E-Mail: k.p.shine@reading.ac.uk;
Tel.: +44-118-378-8405; Fax: +44-118-378-8905.

Received: 13 May 2014; in revised form: 12 June 2014 / Accepted: 24 June 2014 /

Published: 17 July 2014

Abstract: CFC-113a (CF₃CCl₃), CFC-112 (CFCl₂CFCl₂) and HCFC-133a (CF₃CH₂Cl) are three newly detected molecules in the atmosphere that are almost certainly emitted as a result of human activity. It is important to characterise the possible contribution of these gases to radiative forcing of climate change and also to provide information on the CO₂-equivalence of their emissions. We report new laboratory measurements of absorption cross-sections of these three compounds at a resolution of 0.01 cm⁻¹ for two temperatures 250 K and 295 K in the spectral range of 600–1730 cm⁻¹. These spectra are then used to calculate the radiative efficiencies and global warming potentials (GWP). The radiative efficiencies are found to be between 0.15 and 0.3 W·m⁻²·ppbv⁻¹. The GWP for a 100 year time horizon, relative to carbon dioxide, ranges from 340 for the relatively short-lived HCFC-133a to 3840 for the longer-lived CFC-112. At current (2012) concentrations, these gases make a trivial contribution to total radiative forcing; however, the concentrations of CFC-113a and HCFC-133a are continuing to increase. The 2012 CO₂-equivalent emissions,

using the GWP (100), are estimated to be about 4% of the current global CO₂-equivalent emissions of HFC-134a.

Keywords: chlorofluorocarbons; hydrochlorofluorocarbons; absorption cross-section; absorption intensity; radiative efficiency; global warming potential (GWP)

1. Introduction

The emission of halogenated compounds from human activity can cause stratospheric ozone depletion and climate change. Recently, the first atmospheric detection of a further four such halogenated compounds has been reported [1]. The four compounds are CFC-112 (CFCl₂CFCl₂) (with concentrations measured at Cape Grim, Tasmania of 0.44 ppt in late-2012), CFC-112a (CF₂CICCl₃) (0.07 ppt), CFC-113a (CF₃CCl₃) (0.48 ppt) and HCFC-133a (CF₃CH₂Cl) (0.37 ppt). CFC-113a concentrations increased between 1978 and 2012. HCFC-133a in general increased, with an interruption in the increase between 2008 and 2010. CFC-112 concentrations peaked in 1997, and have been falling slowly since then; CFC-112a concentrations (measured since 1999) are believed to have behaved in a similar way. These compounds continue to be emitted as a result of human activity (possibly contravening the United Nations Montreal Protocol on Substances that Deplete the Ozone Layer) [1]. The emission sources are uncertain.

On a molecule-per-molecule basis, such halocarbons are potent greenhouse gases (e.g., [2]). Although at existing concentrations these particular CFCs and HCFCs contribute insignificantly to radiative forcing of climate change, it is necessary to quantify this contribution, particularly for those whose concentrations are increasing, and may become significant in the future. It is also necessary to provide values for metrics such as the Global Warming Potential (GWP) which is used within the Kyoto Protocol to the United Nations Framework Convention on Climate Change for placing emissions of different greenhouse gases on a CO₂-equivalent scale.

This work presents, for the first time, quantitative spectrally-resolved infrared spectra for these new molecules, and the radiative efficiencies and GWPs that result from using these spectra in a radiative transfer model. Although some infrared measurements of these molecules have been published [3–6], these were not reported in the detailed spectrally-resolved form which is required for their incorporation into radiative transfer models.

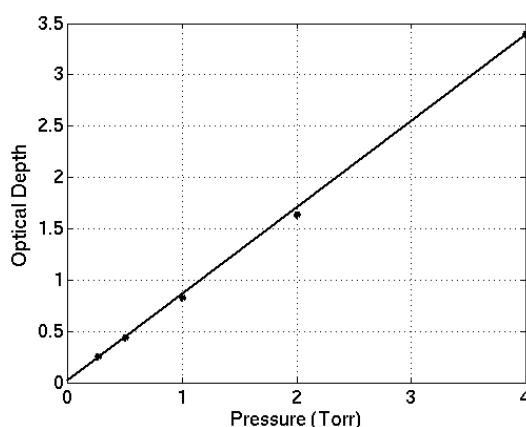
This paper reports new laboratory measurements of the infrared absorption cross-sections of three of these four compounds (Sections 2–4), and presents for the first time calculations of radiative efficiencies (Section 5) and GWPs (Section 6) using these cross-sections together with atmospheric lifetimes recently reported by Laube *et al.* [1].

2. Experimental Setup

Spectra were measured at the Rutherford Appleton Laboratory Molecular Spectroscopy Facility using a Bruker IFS 125 HR Fourier transform spectrometer. Measurements were performed over the wavenumber range of 600–1730 cm⁻¹. The gas was contained in a 5 cm path length stainless-steel

coolable cell with potassium bromide windows. Four platinum resistance thermometers were attached to the outside of the cell and a National Instruments data logger (NI4351) recorded the temperature. A mercury-cadmium-telluride (MCT) detector measured the spectra of sample gas. The spectral resolution of measurements was 0.01 cm^{-1} at some pressures, and 0.015 cm^{-1} at others. Measurements were performed with a pure sample at various gas pressures at 250 K and 295 K. At least two cycles of freeze-pump-thaw were performed to remove any atmospheric contamination from the liquid samples of CFC-112, CFC-112a and CFC-113a; the gas sample of HCFC-133a was used without further purification. Measurements were also made at 295 K in the presence of a broadening gas (artificial air—Air Products zero air, 79.1% nitrogen, and 20.9% oxygen) at different pressures. For these measurements, the required amount of pure gas was admitted to a mixing bulb and artificial air was added up to 1000 Torr. The bulb was left overnight to mix well; the next day the mixture was introduced into the cell for measurements. Pressure was measured by one of three MKS Baratron type 690 (1000, 10 or 1 Torr full scale) with readings logged once a second. The measurements presented here focus on the highest pressure pure gas cases where measurements were made at 0.01 cm^{-1} , as these were the most detailed and the least contaminated by noise (particularly at lower wavenumbers where the MCT detector response decreases). The lower pressure measurements were mostly used to ensure that the peak absorption varied linearly with absorber amount, to ensure that saturation of signal was not a problem for these higher pressure cases. The maximum value of the optical depth (at 1227 cm^{-1}) of CFC-113a for different sample gas pressure is examined (Figure 1) which confirms a linear increase with zero intercept and demonstrates there is no saturation during the experiments.

Figure 1. Maximum value of optical depth of CFC-113a *versus* pressure at 1227 cm^{-1} .



3. Data Analysis

The absorption spectrum was measured in two steps: the background spectrum was obtained using a cell which was evacuated to less than 10^{-3} Torr and then the cell was filled with the sample gas up to the specified pressure and the second spectrum was obtained. This method has been widely used in the past (e.g., [7,8]). From the measured value of $I(\nu)$ (background intensity with the evacuated cell) and $I_0(\nu)$ (intensity with sample), where ν is wavenumber, and using the Beer-Lambert-Bouguer Law $I(\nu) = I_0(\nu)\exp[-\tau(\nu)]$, the optical depth (absorbance) $\tau(\nu)$ can be derived using

$$\tau(\nu) = \log_e \left[\frac{I_0(\nu)}{I(\nu)} \right] \quad (1)$$

The absorption cross-section can then be derived using

$$\tau(\nu) = \sigma(\nu)nL \quad (2)$$

where L is the path length in (cm), $\sigma(\nu)$ is the absorption cross-section in ($\text{cm}^2 \cdot \text{molecule}^{-1}$) and n is the number density of the absorbing molecule in ($\text{molecule} \cdot \text{cm}^{-3}$). The value of n is obtained from $n = (273.13 \times PL_0)/(1013.0 \times T)$ where P is the pressure of the absorber in hPa, T is the gas temperature in Kelvin and L_0 is Loschmidt's number $2.69 \times 10^{19} \text{ molecule} \cdot \text{cm}^{-3}$. The integrated absorption cross-section S is derived by integration of the absorption cross-section σ over the whole range of wavenumbers ν

$$S = \int_{\text{lower}}^{\text{upper}} \sigma(\nu) d\nu \quad (3)$$

Measurement uncertainties are estimated for the higher pressure cases which are of most importance here: path length (less than $\pm 0.1\%$), temperature ($\pm 0.5\%$), pressure ($\pm 2\%$), sample purity ($\pm 1\%$) and noise in the spectra ($\pm 1.5\%$). A baseline correction was not necessary. The overall root-sum-square error is $\pm 2.7\%$. For lower pressures, the smaller absorption increases the relative contribution of the noise significantly; these measurements are less reliable for deriving S . The absorption between the main bands was set to zero to exclude contamination of S from noise in these regions.

Absorption cross-sections for each gas are provided in digital form in the supplementary information.

4. Infrared Absorption Cross-Section

4.1. CFC-113a

Spectra for pure CFC-113a were obtained at 295 K for pressures from 0.267 to 4 Torr. Figure 2a presents the spectrum at 2.7 Torr taken at 0.01 cm^{-1} resolution. It shows five distinct bands located in three main regions: $703\text{--}725 \text{ cm}^{-1}$, $840\text{--}920 \text{ cm}^{-1}$ and $1180\text{--}1290 \text{ cm}^{-1}$. These results agree well with the findings of Nielsen *et al.* [3] and Olliff and Fischer [4]. The bands centred at 1227 and 1255 cm^{-1} have been associated with C-F stretching, the band at 909 cm^{-1} with C-C stretching and bands at 859 and 714 cm^{-1} with C-Cl stretching [3].

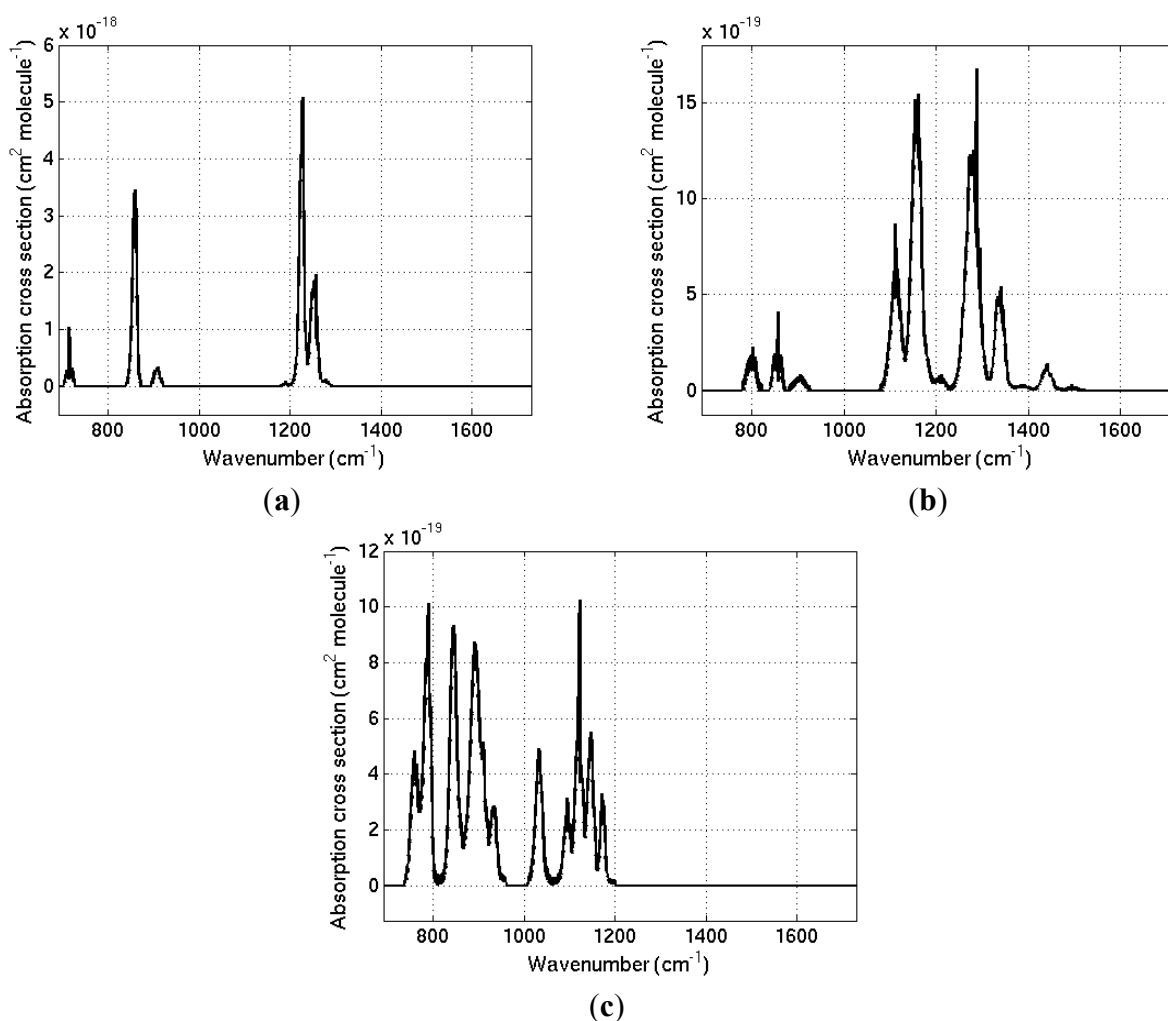
For the pure gas sample at 2.7 Torr, $S = 1.35 \pm 0.036 \times 10^{-16} \text{ cm}^2 \cdot \text{molecule}^{-1} \cdot \text{cm}^{-1}$, about 4% larger than the result of Olliff and Fischer [4]. Measurements at different pressures do not change the value of S by more than 3.5%, and hence the measurements at different pressures are within the stated experimental uncertainties. In the three sub-bands S is $4.97 \times 10^{-18} \text{ cm}^2 \cdot \text{molecule}^{-1} \cdot \text{cm}^{-1}$ ($703\text{--}725 \text{ cm}^{-1}$), $4.30 \times 10^{-17} \text{ cm}^2 \cdot \text{molecule}^{-1} \cdot \text{cm}^{-1}$ ($840\text{--}920 \text{ cm}^{-1}$) and $8.76 \times 10^{-17} \text{ cm}^2 \cdot \text{molecule}^{-1} \cdot \text{cm}^{-1}$ ($1180\text{--}1290 \text{ cm}^{-1}$).

Measurements at 250 K and 1.98 Torr show that S is within 3% of the 295 K measurements, and again within the stated uncertainties. Although S is little affected by temperature, the absorption band features change slightly. There is an increase in structure and the Q branch of absorption bands becomes sharper and more intense at lower temperature. The presence of the broadening gas was

found to change the value of S by less than 1.5% compared to the pure sample, which is again within the experimental uncertainties. A similar lack of sensitivity to broadening gas has been found for other similar molecules (see, for example, the measurements of Smith *et al.* [7] for HFC-134 and HFC-143a).

These CFC-113a measurements can be compared with those of its isomer CFC-113 ($\text{CCl}_2\text{FCClF}_2$), the third most abundant chlorofluorocarbon in the atmosphere [9]. Recent laboratory measurements [10] indicate that S is about $1.35 \times 10^{-16} \text{ cm}^2 \cdot \text{molecule}^{-1} \cdot \text{cm}^{-1}$ at 283 K, which is very similar to our value for CFC-113a. However, the spectral structure of CFC-113 is quite different, with 6 rather than 4 distinct bands between 800 and 1300 cm^{-1} . The origin of this difference is that for CFC-113a each carbon atom has bonds with either all fluorine or all chlorine atoms, while for CFC-113, the bonds with each carbon atom are a mixture of chlorine and fluorine. More specifically, CFC-113 (which has conformations with point group C_1 and C_s) has only non-degenerate vibrations accessible by allowed transitions, while CFC-113a (which belongs to the C_{3v} point group) gives rise to degenerate (E) vibrations, along with an A_2 vibration that cannot be accessed in allowed transitions.

Figure 2. Absorption spectrum at 295 K for: (a) 2.7 Torr of CFC-113a; (b) 6.96 Torr of HCFC-133a; and (c) 8.1 Torr of a 90.8%/9.2% mixture of CFC-112/112a within the range of 690–1600 cm^{-1} .



4.2. HCFC-133a

The spectrum of pure HCFC-133a was measured at 295 K for pressures from 0.94 to 9.53 Torr. Figure 2b shows its spectrum for a pressure of 6.96 Torr taken at 0.01 cm^{-1} resolution. There is a series of bands between 690 and 1730 cm^{-1} that are divided into 2 main regions: $780\text{--}920\text{ cm}^{-1}$ and $1070\text{--}1530\text{ cm}^{-1}$.

The different absorption features have been associated by [5] as follows: C-Cl stretching (801 cm^{-1}), C-C stretching (855 cm^{-1}), CH_2 wagging and rocking (905 and 1110 cm^{-1}), C-F stretching (1159 , 1267 , 1277 cm^{-1}) and $-\text{CH}_2$ deformation and twisting (1339 and 1443 cm^{-1}).

For the pure gas sample at 6.96 Torr, $S = 1.21 \pm 0.033 \times 10^{-16}\text{ cm}^2\cdot\text{molecule}^{-1}\cdot\text{cm}^{-1}$. For measurements at different pressures S changes by no more than 5.5%. In the two distinct regions identified above S is $9.02 \times 10^{-18}\text{ cm}^2\cdot\text{molecule}^{-1}\cdot\text{cm}^{-1}$ ($780\text{--}920\text{ cm}^{-1}$) and $1.12 \times 10^{-16}\text{ cm}^2\cdot\text{molecule}^{-1}\cdot\text{cm}^{-1}$ ($1070\text{--}1530\text{ cm}^{-1}$). We are unaware of any previous literature to compare our values with.

Measurements at 250 K and 4.99 Torr show that S is within 1% of the value at 295 K, and so within the stated experimental uncertainty. Although S is little affected by temperature, the features of absorption bands change slightly in the same way as found for CFC-113a in the previous subsection. The presence of the broadening gas was found to change the value of S by less than 1.7% compared to the pure sample, which is again within the experimental uncertainties.

4.3. CFC-112/CFC-112a

Separate samples of CFC-112 and CFC-112a are not available to us under Montreal Protocol's import restrictions. Measurements were therefore limited to the only available mixture of CFC-112 (90.8%) and CFC-112a (9.2%). The composition of this mixture is similar to the ratio found in the atmosphere [1], so that the measured cross-section could then be considered representative of this mixture. We analysed theoretical calculations (DFT, B3LYP) of the cross-sections of CFC-112 and CFC-112a (performed by David Nutt, University of Reading, personal communication, 2012) to see whether these could guide the derivation of separate cross-sections for the two species, by allowing us to attribute specific bands to each of the molecules. Although previous work had indicated that such *ab initio* calculations worked reasonably well for the perfluorocarbons [11], the calculations were insufficiently accurate for use to derive separate CFC-112 and CFC-112a cross-sections, and so this method was not pursued further here.

The absorption spectrum for the mixture of CFC-112 (90.8%) and CFC-112a (9.2%) at 8.10 Torr and 295 K, taken at 0.01 cm^{-1} resolution, is shown in Figure 2c. The bands are centred in two regions: $740\text{--}960\text{ cm}^{-1}$ and $1010\text{--}1200\text{ cm}^{-1}$. For this sample, $S = 1.12 \pm 0.03 \times 10^{-16}\text{ cm}^2\cdot\text{molecule}^{-1}\cdot\text{cm}^{-1}$ and in the two regions S is $7.46 \times 10^{-17}\text{ cm}^2\cdot\text{molecule}^{-1}\cdot\text{cm}^{-1}$ ($740\text{--}960\text{ cm}^{-1}$) and $3.75 \times 10^{-17}\text{ cm}^2\cdot\text{molecule}^{-1}\cdot\text{cm}^{-1}$ ($1010\text{--}1200\text{ cm}^{-1}$). In previous work, values of S of 1.08×10^{-16} and $1.06 \times 10^{-16}\text{ cm}^2\cdot\text{molecule}^{-1}\cdot\text{cm}^{-1}$ were obtained for CFC-112 and CFC-112a separately [6]; by combining these individual values of S to give a value appropriate for the mixture used here, our results agree with these older measurements within 4%. A more detailed comparison of absorption features is not possible as [6] did not present resolved spectra. The measurements at different pressures

do not change the value of S by more than 3.5%, which is within the stated uncertainty of our measurements.

Measurements at 250 K and 1.88 Torr show that S is within 1% of the measurements at 295 K, again within the uncertainty of our measurements. As with the other gases reported here, S is little affected by temperature. The presence of the broadening gas was found to change the value of S by less than 2% compared to the pure sample, and so within the uncertainty of our measurements.

5. Radiative Efficiency

Radiative efficiencies (RE) ($\text{W}\cdot\text{m}^{-2}\cdot\text{ppbv}^{-1}$) are calculated using an updated version of a narrow-band radiative transfer model (NBM) [12], broadly following the methodology of Sihra *et al.* [13]. Three cloudy-sky atmospheres (see Appendix B of Freckleton *et al.* [14]) are used to represent the tropics and extratropics, and stratospheric temperature adjustment is applied (which increases RE by about 10% for the molecules presented here). The halocarbon cross-sections are averaged onto the NBM's 10 cm^{-1} grid. Calculations are performed for halocarbon mixing ratios of 0.1 ppb, to ensure they are in their linear limit; these are multiplied by 10 to yield RE. HITRAN2004 [15] provides the spectral line data for water vapour, ozone, carbon dioxide, methane and nitrous oxide. Water vapour, ozone and cloud profiles are specified for each atmosphere [14]. Other gases are assumed to be well-mixed using 2010 concentrations of 389 ppm for CO_2 , 1800 ppb for CH_4 , and 323 ppb for N_2O . The 2010 concentration of main greenhouse gases is obtained from [16]. A fast method for calculating instantaneous RE has recently been presented [2], based on line-by-line calculations, which is an update to a previously-available method [17] but at finer spectral resolution. Using this fast method the instantaneous RE for CFC-113a and CFC-112 is within 0.5%, and HCFC-133a is within 1.5%, of the instantaneous RE calculated using the NBM.

Table 1. Radiative efficiencies, mixing ratios in late-2012, present-day radiative forcings, atmospheric lifetimes, GWPs (for time horizons of 20, 100 and 500 years) and the GTP for a time horizon of 50 years, for the 3 gases considered here.

Gas	Radiative Efficiency ($\text{W}\cdot\text{m}^{-2}\cdot\text{ppbv}^{-1}$)	Mixing Ratio (pptv)	Radiative Forcing ($\text{W}\cdot\text{m}^{-2}$)	Lifetime (years)	GWP (20)	GWP (100)	GWP (500)	GTP (50)
CFC-113a	0.23	0.48	1.10×10^{-4}	51	4590	3310	1100	3920
CFC-112	0.29	0.44	1.28×10^{-4}	51	5320	3840	1270	4540
HCFC-133a	0.15	0.37	5.60×10^{-5}	4.3	1220	340	96	74

Halocarbons are not well-mixed in the atmosphere because of stratospheric and tropospheric removal processes. There is no unique way of accounting for the effect of this on RE, especially for shorter lived species such as HCFC-133a, as the inhomogeneity depends on emission location. We applied the steady-state correction factors derived by Hodnebrog *et al.* [2] which assume the same geographical distribution as current emissions of CFC-11, using the lifetimes derived by Laube *et al.* [1] (see Table 1). The multiplicative factors to account for the inhomogeneity are 0.95 for the three CFCs and 0.91 for HCFC-133a, but the uncertainty in the correction factor for the shorter-lived HCFC-133a is greater, as it is more dependent on assumptions as to where it is emitted. Table 1 presents the

final RE values. It also shows that the radiative forcing for current (2012) concentrations given by Laube *et al.* [1] is trivially small (of order $0.1 \text{ mW}\cdot\text{m}^{-2}$), although, as noted earlier, the concentrations of CFC-113a and HFC-133a were found to be still increasing [1] and so could become significant if this growth were to be sustained.

We adopt the Hodnebrog *et al.* [2] uncertainties (5%–95% confidence range) which are about 13% for CFC-113a and CFC-112 and approximately 23% for HCFC-133a because of its less certain lifetime correction.

6. Global Warming Potentials

The GWP is one method for placing the climate effect of emissions of different gases on a common CO_2 -equivalent scale (e.g., [18]). It is the time-integrated radiative forcing of a pulse emission of a unit mass of gas, integrated over a time horizon H , divided by the same quantity for a pulse emission of the same mass of CO_2 . The GWP for $H = 100$ years (GWP (100)) is used by the Kyoto Protocol. The absolute GWP for CO_2 used here are from [2] and are 2.495×10^{-14} , 9.171×10^{-14} and $32.17 \times 10^{-14} \text{ W}\cdot\text{m}^{-2}\cdot\text{year} (\text{kgCO}_2)^{-1}$ for the horizons of 20, 100 and 500 years, respectively, and are based on emissions with a 2011 background of CO_2 and the impulse response function of Joos *et al.* [19]. Table 1 presents the GWP for $H = 20, 100$ and 500 years. An alternative emission metric, the Global Temperature change Potential (GTP) [20] computes the temperature change at some time H after a pulse emission (relative to an emission of the same mass of CO_2). To calculate the GTP it is necessary to represent the surface temperature response to the radiative forcing pulse, and values are sensitive to this representation (e.g., [20]). We use the methodology in Hodnebrog *et al.* [2] and present the GTP for $H = 50$ years for illustration.

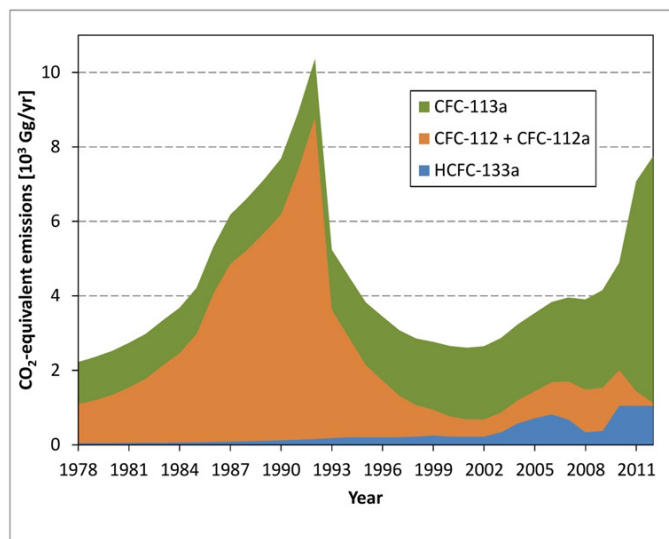
The GWP and GTP values in Table 1 are typical of similar molecules, with HCFC-133a being the smallest, mostly on account of its much shorter lifetime, but also because of its lower RE. The GTP (50) is similar to the GWP (100) for the two CFCs, but much smaller for HCFC-133a, on account of the short lifetime (the climate system retains relatively little memory of the short-lived pulse of radiative forcing following the emission). The GWP (100) and GTP (50) for CFC-113a are only 65%–70% of the values found for its isomer CFC-113 [2] on account of both the larger RE for CFC-113 ($0.3 \text{ W}\cdot\text{m}^{-2}\cdot\text{ppbv}^{-1}$) and its longer lifetime (85 years).

Hodnebrog *et al.* [2] estimated the GWP uncertainties (5%–95% confidence range) for CFC-11 (which has a lifetime of 45 years) to be about 25%, 40% and 50% for a $H = 20, 100,$ and 500 years respectively, and these uncertainty estimates are appropriate for CFC-113a and CFC-112. They did not present detailed error estimates for shorter-lived species, but noted that gases with lifetimes of less than 5 years (and hence HCFC-133a is in this category) would have errors approximately double those estimated for CFC-11.

Using estimates of the 2012 emissions [1] of CFC-113a, CFC-112, and HCFC-133a, which are 2, 0.01, and $3.10 \text{ Gg}\cdot\text{year}^{-1}$ respectively, yields CO_2 -equivalent emissions of 6620, 38, and $1050 \text{ Gg}\cdot\text{year}^{-1}$ respectively, using the GWP (100) given in Table 1. The time variation of the CO_2 -equivalent emissions is shown in Figure 3. For comparison, the estimated 2010 CO_2 -equivalent global emissions of the most-abundant HFC in the atmosphere, HFC-134a, are $195,000 \text{ Gg}\cdot\text{year}^{-1}$ using the emission estimates and GWP (100) from [18]; hence the emissions of the new species considered here constitute, in

CO₂-equivalent terms, about 4% of global HFC-134a emissions and about 0.02% of the global CO₂ emissions from fossil-fuels and other industrial sources [18]. At their peak in 1992 [1], the estimated emissions of CFC-112 were about 2.2 Gg·year⁻¹, or 8640 Gg·year⁻¹ in CO₂-equivalent terms.

Figure 3. Time series of CO₂ equivalent emissions of the CFC-113a, HFC-133a, CFC-112 and CFC-112a, using the emission values in [1] and the GWP (100) values given in Table 1.



7. Conclusions

Detailed absorption cross-sections of three newly detected gases in the atmosphere, CFC-113a, HCFC-133a and mixture of CFC-112/CFC-112a (predominantly CFC-112), are presented at 295 K over the wavenumber range of 690–1730 cm⁻¹. These are used to calculate, for the first time, radiative efficiencies and global warming potentials for the three gases. This allows the quantification of the radiative forcing due to these gases and the CO₂-equivalence of their emissions. Although their current contribution to radiative forcing is trivial, they are nevertheless powerful greenhouse gases on a molecule-per-molecule basis and their GWP (100) values range from 340 to 3380. It would be desirable to produce separate values of absorption cross-section, radiative efficiency and GWP for CFC-112a, if a pure sample of that gas becomes available.

Acknowledgments

We thank David Nutt for providing preliminary *ab initio* cross-section calculations. The Natural Environment Research Council supported the measurements at the RAL Molecular Spectroscopy Facility and the Research Fellowships via grants NE/F015585/1 & NE/I021918/1. We thank the reviewers for many helpful comments.

Author Contributions

The work presented here was carried out in a collaboration between all authors. The study was conceived by Johannes C. Laube, George Marston and Keith P. Shine, with advice from Kevin M. Smith, Robert McPheat, with input from Kevin M. Smith and Johannes C. Laube, performed the laboratory

measurements. The spectroscopic data was analysed by Maryam Etminan, with input from Eleanor J. Highwood, George Marston, Robert McPheat, Keith P. Shine and Kevin M. Smith. Maryam Etminan and Keith P. Shine performed the radiative and metric calculations with input from Johannes C. Laube and Eleanor J. Highwood. The writing was led by Maryam Etminan and Keith P. Shine, and all authors contributed to reviewing and revising the text.

Conflicts of Interest

The authors declare no conflict of interest.

References

1. Laube, J.C.; Newland, M.J.; Hogan, C.; Brenninkmeijer, C.A.M.; Fraser, P.J.; Martinerie, P.; Oram, D.E.; Reeves, C.E.; Röckmann, T.; Schwander, J.; *et al.* Newly detected ozone depleting substances in the atmosphere. *Nat. Geosci.* **2014**, *7*, 266–269.
2. Hodnebrog, O.; Etminan, M.; Fuglestvedt, J.S.; Marston, G.; Myhre, G.; Nielsen, C.J.; Shine, K.P.; Wallington, T.J. Global warming potentials and radiative efficiencies of halocarbons and related compounds: A comprehensive review. *Rev. Geophys.* **2013**, *15*, 300–378.
3. Nielsen, J.R.; Liang, C.Y.; Smith, R.M.; Smith, D.C. Infrared and raman spectra of ethanes. V. The series CF₃CF₃, CF₃CF₂Cl, CF₃CFCl₂ and CF₃CCl₃. *J. Chem. Phys.* **1953**, *21*, 383–393.
4. Olliff, M.P.; Fischer, G. Integrated band intensities of 1,1,1-trichlorotrifluoroethane, CFC 113a, and 1,1,2-trichlorotrifluoroethane, CFC113. *Spectrochim. Acta Part A: Mol. Spectrosc.* **1992**, *48*, 229–235.
5. Nielsen, J.R.; Liang, C.Y.; Smith, D.C. Infrared and raman spectra of ethanes. VI. The series CF₃CH₃, CF₃CH₂Cl, CF₃CHCl₂ and CF₃CCl₃. *J. Chem. Phys.* **1953**, *21*, 1060–1069.
6. Olliff, M.P.; Fischer, G. Integrated absorption intensities of haloethanes and halopropanes. *Spectrochim. Acta Part A: Mol. Spectrosc.* **1994**, *50*, 2223–2237.
7. Smith, K.; Newnham, D.; Page, M.; Ballard, J.; Duxbury, G. Infrared absorption cross-section and integrated absorption intensities of HFC-134 and HFC-143a vapour. *J. Quant. Spectrosc. Radiat. Transf.* **1998**, *59*, 437–451.
8. Ballard, J.; Knight, R.J.; Newnham, D.A. Infrared absorption cross-section and integrated absorption intensities of perfluoroethane and cis-perfluorocyclobutane. *J. Quant. Spectrosc. Radiat. Transf.* **2000**, *66*, 199–212.
9. WMO. *Scientific Assessment of Ozone Depletion 2010*; Global Ozone Research and Monitoring Project—Report 52; World Meteorological Organization: Geneva, Switzerland, 2011.
10. Le Bris, K.; Pandharpurkar, R.; Strong, K. Mid-infrared absorption cross-section and temperature dependence of CFC-113. *J. Quant. Spectrosc. Radiat. Transf.* **2011**, *112*, 1280–1285.
11. Bravo, I.; Aranda, A.; Hurley, M.D.; Marston, G.; Nutt, D.R.; Shine, K.P.; Smith, K.; Wallington, T.J. Infrared absorption spectra, radiative efficiencies, and global warming potentials of perfluorocarbons: Comparison between experiment and theory. *J. Geophys. Res.* **2010**, doi:10.1029/2010JD014771.
12. Shine, K.P. On the cause of the relative greenhouse strength of gases such as the halocarbons. *J. Atmos. Sci.* **1991**, *48*, 1513–1518.

13. Sihra, K.; Hurley, M.D.; Shine, K.P.; Wallington, T.J. Updated radiative forcing estimates for 65 halocarbons and nonmethane hydrocarbons. *J. Geophys. Res.* **2001**, *106*, 20493–20505.
14. Freckleton, R.S.; Highwood, E.J.; Shine, K.P.; Wild, O.; Law, K.S.; Sanderson, M.G. Greenhouse gas radiative forcing: Effects of averaging and inhomogeneities in trace gas distribution. *Quart. J. Roy. Meteorol. Soc.* **1998**, *124*, 2099–2127.
15. Rothman, L.S.; Jacquemart, D.; Barbe, A.; Benner, D.C.; Birk, M.; Brown, L.R.; Carleer, M.R.; Chacke, C., Jr.; Chance, K.; Coudert, L.H.; *et al.* The HITRAN 2004 molecular spectroscopic database. *J. Quant. Spectrosc. Radiat. Transf.* **2005**, *96*, 139–204.
16. U.S. Department of Commerce/National Oceanic and Atmospheric Administration/NOAA Research. NOAA's Annual Greenhouse Gas Index (An Introduction). Available online: <http://www.esrl.noaa.gov/gmd/aggi/> (accessed on 25 June 2014).
17. Pinnock, S.; Hurley, M.D.; Shine, K.P.; Wallington, T.J.; Smyth, T.J. Radiative forcing of climate by hydrochlorofluorocarbons and hydrofluorocarbons. *J. Geophys. Res.* **1995**, *100*, 23227–23238.
18. IPCC. The physical science basis contribution of working group I to the fifth assessment report of the intergovernmental panel on climate change. In *Climate Change 2013*; Stocker, T.F., Qin, D., Plattner, G.-K., Tignor, M., Allen, J., Boschung, A., Nauels, J., Xia, Y., Bex, V., Midgley, P.M., Eds.; Cambridge University Press: Cambridge, UK, 2013.
19. Joos, F.; Roth, R.; Fuglestedt, J.S.; Peters, G.P.; Enting, I.G.; von Bloh, W.; Brovkin, V.; Burke, E.J.; Eby, M.; Edwards, N.R.; *et al.* Carbon dioxide and climate impulse response functions for the computation of greenhouse gas metrics: A multi-model analysis. *Atmos. Chem. Phys.* **2013**, *13*, 2793–2825.
20. Shine, K.P.; Fuglestedt, J.S.; Hailemariam, K.; Stuber, N. Alternatives to the global warming potential for comparing climate impacts of emissions of greenhouse gases. *Clim. Chang.* **2005**, *68*, 281–302.